Resonances in Heterogeneous Dielectric Bodies with Rotational Symmetry—Volume Integral-Equation Formulation

Andrzej A. Kucharski

***Abstract*—In this paper, a method of determining resonant frequencies and field distributions in heterogeneous bodies of revolution is presented. A volume electric-field integral equation is put into modal form, and then discretized with the method of moments. In the solution process, specially defined divergenceless basis functions are used, which reduces the number of unknowns and makes the algorithm more efficient. The identification of resonances is particularly easy because of the mode separation included in the formulation.**

***Index Terms*—Dielectric resonators, integral equations, method of moments.**

I. Introduction

DIELECTRIC resonators [1] are widely used in microwave circuits because of their low cost, small size, and temperature stability. In recent years, they have been also often utilized as so-called resonant dielectric cavity antennas [2], [3]. Although most of solutions concern homogeneous resonator structures, recent efforts have been devoted to inhomogeneous ones, mainly because of searching for bandwidth enhancement techniques [4], [5].

A great number of methods have been proposed for analysis of dielectric resonators. Those techniques include perfect magnetic conducting (PMC) wall methods [1], [2], mode-matching techniques [6], surface integral-equation methods [7], [8], T-matrix approach [9], and many others. Some of known approaches are limited to closed or partially shielded geometries, other are well suited for homogeneous structures or resonators consisting of a small number of homogeneous regions. Recently, Viola [10] has given a theoretical background for efficient modeling of highly heterogeneous bodies of revolution (BOR's) using the method-of-moments (MoM) techniques. However, his attitude is not well suited for dealing with step discontinuities in dielectric permittivity profiles.

In this paper, a simple technique for dealing with heterogeneous open (isolated) structures with rotational symmetry is presented. The technique is based on the volume integral-equation (VIE) formulation and modal decomposition of the problem.

Manuscript received June 4, 1998. This work was supported in part by the State Committee for Scientific Research of Poland under Grant 8T11D02311.

The author is with the Radio Department, Institute of Telecommunications and Acoustics, Wroclaw University of Technology, 50–370 Wroclaw, Poland.

Publisher Item Identifier S 0018-9480(00)03747-9.

II. Method of Calculations

A. Modal VIE

Let us assume that a body with rotational symmetry is placed in a free-space environment where no incident fields exist. We are interested in finding nonzero field solutions to Maxwell equations for this particular case. To do so, we start with the equivalence principle, and describe the electric field inside the body with polarization current

$$\mathbf{J}(\mathbf{r}) = j\omega\Big[\hat{\varepsilon}(\mathbf{r}) - \varepsilon_0\Big]\mathbf{E}(\mathbf{r}). \tag{1}$$

where $\hat{\varepsilon}(\mathbf{r}) = \varepsilon(\mathbf{r}) - j\sigma(\mathbf{r})/\omega$; ε and σ are the medium permittivity and conductivity at position $\mathbf{r}$.

The polarization current distribution in the body is related to the electric field in the whole space by the well-known mixed-potential integral equation (MPIE) [11]. Following [12], the MPIE can be put into modal form by expanding all quantities involved into Fourier series in azimuthal component (m denotes the number of the azimuthal mode)

$$\mathbf{E}_m(\rho, z) + j\omega\mathbf{A}_m(\rho, z) + \nabla_m\Phi_m(\rho, z) = 0 \tag{2}$$

where

$$\mathbf{A}_m = \frac{\mu_0}{4\pi}\int_T \bar{\bar{\Gamma}}_m\mathbf{J}_m\rho'\,dt' \tag{3}$$

$$\begin{aligned}\bar{\bar{\Gamma}}_m &= \begin{bmatrix} \Gamma^m_{\rho\rho} & \Gamma^m_{\rho z} & \Gamma^m_{\rho\phi} \\ \Gamma^m_{z\rho} & \Gamma^m_{zz} & \Gamma^m_{z\phi} \\ \Gamma^m_{\phi\rho} & \Gamma^m_{\phi z} & \Gamma^m_{\phi\phi} \end{bmatrix} \\ &= \begin{bmatrix} \dfrac{G_{m-1}+G_{m+1}}{2} & 0 & \dfrac{G_{m-1}-G_{m+1}}{2j} \\ 0 & G_m & 0 \\ \dfrac{G_{m+1}-G_{m-1}}{2j} & 0 & \dfrac{G_{m-1}+G_{m+1}}{2} \end{bmatrix}.\end{aligned} \tag{4}$$

In the above formulas, vector components are taken in the (ρ, z, ϕ) order in usual cylindrical coordinates. The integration in (3) is on the transverse (ρ, z) surface of the BOR.

The modal scalar potential is defined as

$$\Phi_m = \frac{1}{4\pi\varepsilon_0}\int_T q_m G_m\rho'\,dt' \tag{5}$$

where the electric charge density q_m is related to the current $\mathbf{J}_m$ through the continuity equation

$$q_m = -\frac{1}{j\omega}\nabla_m \cdot \mathbf{J}_m = -\frac{1}{j\omega}\left[\frac{1}{\rho'}\frac{\partial(\rho' J_m^\rho)}{\partial\rho} + \frac{\partial J_m^z}{\partial z} + \frac{jm}{\rho'}J_m^\phi\right]. \quad (6)$$

The harmonic gradient operator is defined as

$$\nabla_m \Phi_m = \hat{\rho}\frac{1}{\rho}\frac{\partial(\rho\Phi_m)}{\partial\rho} + \hat{z}\frac{\partial\Phi_m}{\partial z} + \hat{\phi}\frac{jm}{\rho}\Phi_m \quad (7)$$

while the modal Green's function appearing in the above equations is

$$G_m(\rho, z, \rho', z') = \int_0^{2\pi} \frac{e^{-jk_0R}}{R} e^{-jm\alpha}\, d\alpha \quad (8)$$

with

$$R = \sqrt{\rho^2 + \rho'^2 - 2\rho\rho'\cos\alpha + (z-z')^2} \quad (9)$$

$$k_0 = \omega\sqrt{\varepsilon_0\mu_0} = 2\pi/\lambda_0. \quad (10)$$

The following interesting features of (2) can be found for the case $m = 0$.

1) There is no charge associated with the azimuthal field components [see (6)].
2) The modal gradient operator has no azimuthal component [see (7)].
3) $G_{-1} = G_1$ in (4), thus, off-axis matrix components disappear.

From the above, we can draw the conclusion that EFIE's for transverse and azimuthal components are, in this case, decoupled, describing TM_{0n} and TE_{0n} resonance modes, respectively. For $m \neq 0$, (2) does not exhibit such features, which results in a hybrid nature of associated resonances (hybrid electromagnetic (HEM) modes in common notation).

B. Basis and Testing Functions

As the unknown quantity, we choose the electric flux density $\mathbf{D}$ [11]. In order to algebraize (2), we expand $\mathbf{D}$ into a linear combination of basis functions defined on the transverse surface of the body. Basis function for HEM modes are defined as follows (see Fig. 1).

1) ρ-type functions:

$$\mathbf{g}_{mi}(\rho, z) = \begin{cases} \hat{\rho}\frac{1}{\rho}\frac{(\rho - \rho_i^+)}{a_i^+} - \hat{\phi}\frac{1}{jma_i^+}, & \rho \in (\rho_i^+, \rho_i); \\ & z \in \left(z_i^1, z_i^2\right) \\ \hat{\rho}\frac{1}{\rho}\frac{(\rho_i^- - \rho)}{a_i^-} + \hat{\phi}\frac{1}{jma_i^-}, & \rho \in (\rho_i, \rho_i^-); \\ & z \in \left(z_i^1, z_i^2\right) \\ 0, \quad \text{otherwise.} \end{cases} \quad (11)$$

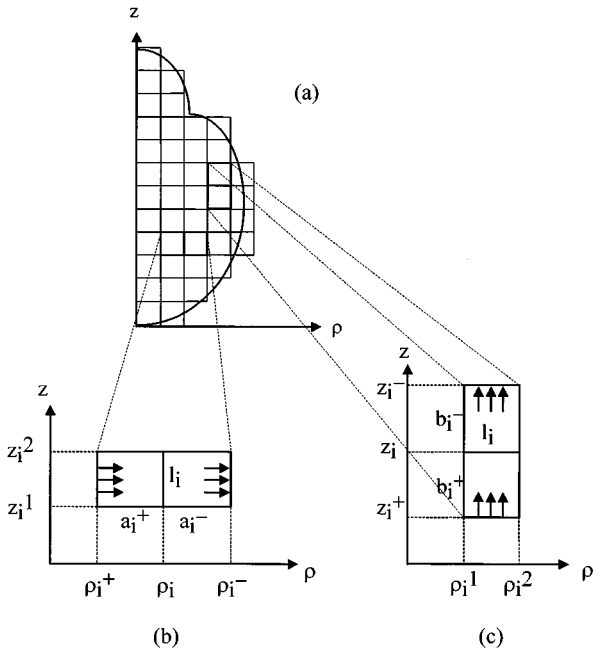

Fig. 1. Discretization of the transverse plane of the body. (a) Geometrical parameters associated with rectangular basis functions. (b) ρ-type. (c) z-type.

2) z-type functions:

$$\mathbf{h}_{mi}(\rho, z) = \begin{cases} \hat{z}\frac{(z - z_i^+)}{b_i^+} - \hat{\phi}\frac{\rho}{jmb_i^+}, & \rho \in \left(\rho_i^1, \rho_i^2\right); \\ & z \in (z_i^+, z_i) \\ \hat{z}\frac{(z_i^- - z)}{b_i^-} + \hat{\phi}\frac{\rho}{jmb_i^-}, & \rho \in \left(\rho_i^1, \rho_i^2\right); \\ & z \in (z_i, z_i^-) \\ 0, \quad \text{otherwise.} \end{cases} \quad (12)$$

For transverse-field components, we use well-known rooftop basis functions, which are defined on pairs of rectangles. The azimuthal component is incorporated into "hybrid" basis function definition with the use of Gauss' law. One can check with (6) that the functions of (11) and (12) are divergenceless, which make them useful for dielectric flux density representation. If the internal edge of the basis function is on the body contour, the basis function is defined only on the rectangle interior to T. No basis functions are associated with the edges lying on the z-axis. It is worth noticing that because we do not define separate basis functions for the azimuthal field component, the total number of unknowns is, in this case, reduced.

We have defined two sets of basis functions associated with vertical and horizontal (in terms of Fig. 1) field components. The definitions differ with the $1/\rho$ factor, which is caused by the fact that, in the case of "ρ-type" basis functions, $\rho\mathbf{D}$ was expanded instead of $\mathbf{D}$, which is a typical step [12] in BOR configurations. In the case of "z-type" functions, however, it is not possible because of difficulties associated with the immediate neighborhood of the z-axis.

For the important case of $m = 0$, simple pulse functions were used for the "azimuthal" equation, while functions similar to (11) and (12), but without azimuthal terms (which are, of

TABLE I
COMPARISON OF COMPUTED AND MEASURED RESONANT FREQUENCY RESULTS FOR RESONATOR WITH RADIUS $a = 5.25$ mm, HEIGHT $h = 4.6$ mm, AND $\varepsilon_r = 38$

Mode	Frequency [GHz]			
	Computed – present method	Computed MoM [8]	Measured [7]	Computed T-matrix [9]
TE_{01}	4.861	4.829	4.85	4.9604
TM_{01}	7.594	7.524	7.60	7.5384
HEM_{11}	6.373	6.333	-	6.3450
HEM_{12}	6.657	6.638	6.64	6.6520
HEM_{21}	7.784	7.752	7.81	7.7621

TABLE II
COMPARISON OF COMPUTED AND MEASURED Q FACTOR RESULTS FOR RESONATOR WITH RADIUS $a = 5.25$ mm, HEIGHT $h = 4.6$ mm, AND $\varepsilon_r = 38$

Mode	Q			
	Computed – present method	Computed MoM [8]	Measured (Transmission method) [7]	Computed T-matrix [9]
TE_{01}	40.7	45.8	51	40.819
TM_{01}	73.7	76.8	86	76.921
HEM_{11}	30.4	30.7	-	30.853
HEM_{12}	49.5	52.1	64	50.316
HEM_{21}	329.8	327.1	204	337.66

course, no longer divergenceless), were applied for the case of "transverse" equation.

As the testing functions, the same functions have been chosen (Galerkin procedure) together with the scalar product. All quantities involved such as polarization currents, charges, and fields have been obtained from above electric flux density basis functions.

C. Calculation of Resonant Frequencies

After an algebraization procedure, (2) can be put into the matrix form

$$\mathbf{S}_m|\mathbf{D}_m\rangle = |0\rangle \tag{13}$$

where $\mathbf{S}_m$ is the moment matrix and $|\mathbf{D}_m\rangle$ is a column vector containing electric flux density coefficients for the mth Fourier mode. Matrix equation (13) has nontrivial solutions only when the determinant of the moment matrix $\mathbf{S}_m$ is zero as follows:

$$\det(\mathbf{S}_m) = 0. \tag{14}$$

The search of the roots of (14) should be done in the complex frequency plane, thus giving information on both resonant frequencies and quality (Q) factors of resonances associated with the mode m [3].

When the resonance frequency is known with a satisfying degree of accuracy, the electric-field distributions within the body can be easily calculated within the multiplicative constant [8]. When one is interested in magnetic field distributions or fields outside the body contour, some additional computational effort is needed.

III. VALIDATION OF THE METHOD

The above procedure has been verified by comparison with results given in the literature. First, resonant frequencies and Q factors of the homogeneous cylindrical resonator DRD105UD046 have been calculated. A comparison of results

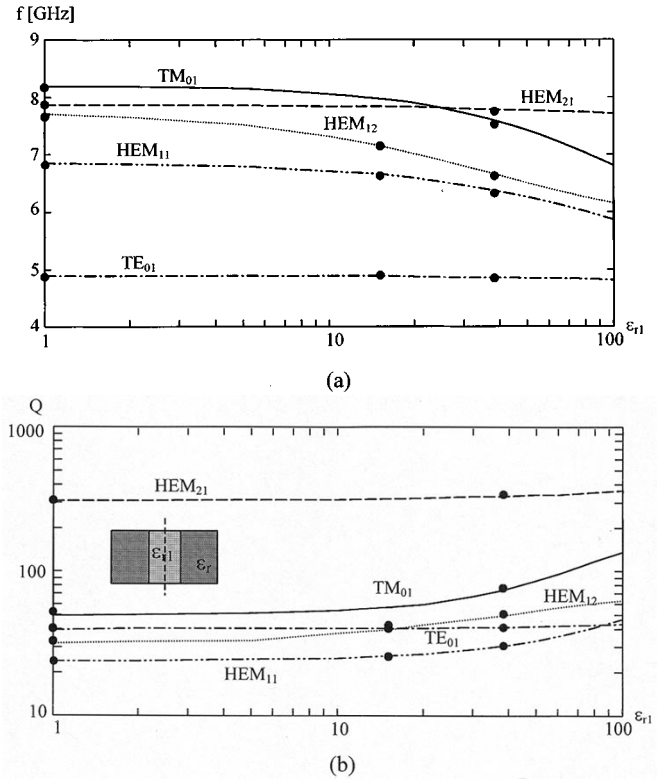

Fig. 2. Resonance frequencies and Q factors of five lower modes of a dielectric inhomogeneous resonator versus permittivity of the inner part. Dimensions: $a = 5.25$ mm, $h = 4.6$ mm, radius of the plug $a_1 = a/4$, $\varepsilon_r = 38$. The circles represent values given in [9]. (a) Resonant frequencies. (b) Q factors.

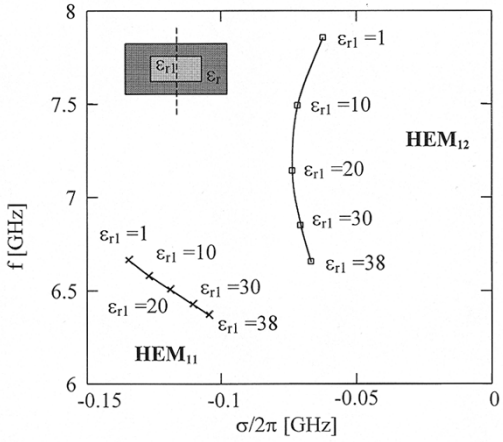

Fig. 3. Changes in the position of complex roots associated with HEM_{11} and HEM_{12} modes caused by decreasing dielectric permittivity of the inner part of the resonator. Dimensions: $a = 5.25$ mm, $h = 4.6$ mm, inner part: $a_1 = 2.625$ mm, $h_1 = 2.3$ mm, $\varepsilon_r = 38$.

is given in Table I (resonant frequencies) and Table II (Q factors). The agreement of results with previously reported values seems to be excellent for resonant frequency values. Differences of results for Q factors are greater; however, it should be remembered that values given in references also differ much from each other as well as from measured results.

The second test concerns an inhomogeneous dielectric resonator with the cylindrical dielectric plug. The dielectric constant of the outer ring is equal to 38, while the dielectric constant of the plug has been changed from 1 (ring resonator) to

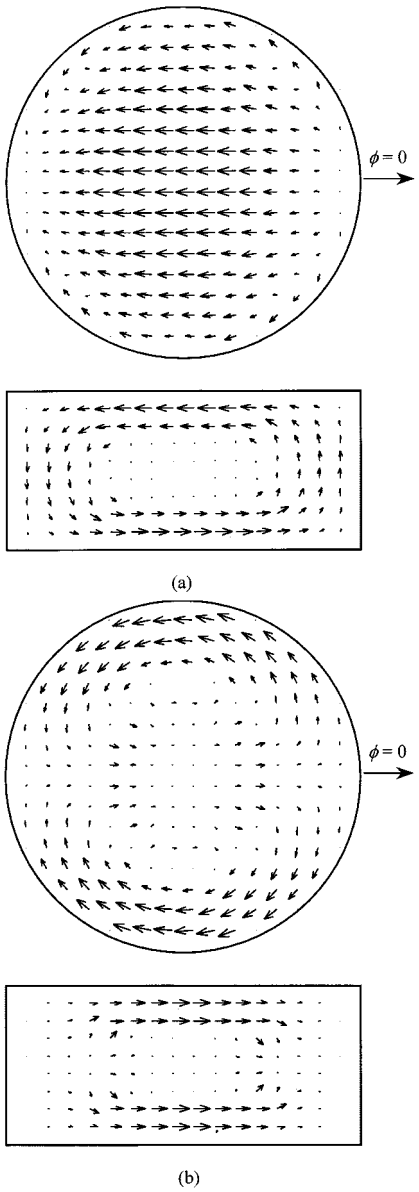

Fig. 4. Electric field inside the nonhomogeneous dielectric resonator, outer part: $a = 5.25$ mm, $h = 4.6$ mm, $\varepsilon_r = 38$, inner part: $a_1 = 2.625$ mm, $h_1 = 2.3$ mm, $\varepsilon_{r1} = 1$. (a) HEM_{11} mode. E-field in plane parallel to and offset from equatorial plane by 2.15 mm (upper figure) and E-field in meridian plane $\phi = 0$ (bottom figure). (b) HEM_{12} mode. E-field in equatorial plane (upper figure) and E-field in meridian plane $\phi = 0$ (bottom figure).

100. The results are given in Fig. 2. Black circles included in the plots correspond to values reported by Zheng [9]. Again, a very good agreement of results has been obtained.

Computational efficiency of the code is comparable to that of a three-dimensional surface integral equation (3-D SIE) algorithms, when homogeneous structures are taken into consideration. For highly heterogeneous bodies, 3-D SIE codes become unacceptably inefficient, while the efficiency of the present method remains almost unchanged. On the other hand, thanks to the reduction of problem dimension, this method allows treatment of situations exceeding the possibilities of 3-D VIE codes [11]. In the above examples, the computation time was 41 s per frequency for model with 136 unknowns; for the model with doubled spatial resolution (528 unknowns), the computation time grew up to 582 s. Computations were performed on a Sun Ultra 1 workstation.

IV. Application Example

Satisfied with the results from the previous section, we can now apply the method for problems involving inhomogeneous bodies. From Table I, it can be seen, that for some modes, resonant frequencies are very close to each other. It means that when one of the modes is chosen as the desired mode of operation, the second one creates a spurious resonance nearby. We will show how this problem could be dealt with in the use of a heterogeneous structure.

Let us consider HEM_{11} and HEM_{12} modes. The difference in resonant frequencies of the modes is less than 5%. However, it can be easily noticed that in the case of the HEM_{11} mode, the electric field is concentrated near the resonator surface [8]. In contrast to this, for the HEM_{12} mode, the field is concentrated in the inner part. This suggests that, by independently changing the dielectric permittivity of the inner and outer parts of the resonator, we probably could change the relative position of both resonances in the complex frequency plane. This possibility has been tested in the configuration shown in the upper left-hand-side corner of Fig. 3. The dielectric constant of the outer part has been left unchanged ($\varepsilon_r = 38$), while that of the inner part has been changed from 38 to 1. From Fig. 3, it can be noted that while the resonant frequency of the HEM_{11} mode is almost unchanged, the resonant frequency of the HEM_{12} mode is moving toward upper values. For the $\varepsilon_{r1} = 1$ case, the resonant frequency of HEM_{11} is about 18% higher than that of the HEM_{12} mode. The electric-field distributions for both modes have been illustrated in Fig. 4.

V. Conclusion

An efficient method of calculating resonances in heterogeneous BOR's has been presented in this paper. The number of unknowns involved in the solution process is greatly reduced via the choice of divergenceless basis functions for nonzero modes. The method results in a very simple resonance identification scheme because TE_{0n}, TM_{0n}, HEM_{1n}, HEM_{2n}, etc. modes can be investigated separately. It is expected that the generalization of the method for the case of a multilayered environment should not present many theoretical difficulties [13].

References

[1] S. B. Cohn, "Microwave bandpass filters containing high-Q dielectric resonators," *IEEE Trans. Microwave Theory Tech.*, vol. MTT-16, pp. 218–227, Apr. 1968.

[2] S. A. Long, M. W. McAllister, and L. C. Shen, "The resonant cylindrical cavity antenna," *IEEE Trans. Antennas Propagat.*, vol. AP-31, pp. 406–412, May 1983.

[3] A. A. Kishk, M. R. Zunoubi, and D. Kajfez, "A numerical study of a dielectric disk antenna above grounded dielectric substrate," *IEEE Trans. Antennas Propagat.*, vol. 41, pp. 813–821, June 1993.

[4] A. A. Kishk, B. Ahn, and D. Kajfez, "Broadband stacked dielectric resonator," *Electron. Lett.*, vol. 25, no. 18, pp. 1232–1233, Aug. 1989.

[5] K. L. Wong and N. C. Chen, "Analysis of a broadband hemispherical antenna with a dielectric coating," *Microwave Opt. Technol. Lett.*, vol. 7, no. 2, pp. 73–76, 1994.

[6] B. Sauviac, P. Guillot, and H. Baudrand, "Rigorous analysis of shielded cylindrical dielectric resonators by dyadic Green's functions," *IEEE Trans. Microwave Theory Tech.*, vol. 42, pp. 1484–1493, Aug. 1994.

[7] A. W. Glisson, D. Kajfez, and J. James, "Evaluation of modes in dielectric resonators using surface integral equation formulation," *IEEE Trans. Microwave Theory Tech.*, vol. MTT-31, pp. 1023–1029, Dec. 1983.
[8] ——, "Computed modal field distributions for isolated dielectric resonators," *IEEE Trans. Microwave Theory Tech.*, vol. MTT-32, pp. 1609–1616, Dec. 1984.
[9] W. Zheng, "Computation of complex resonant frequencies of isolated composite objects," *IEEE Trans. Microwave Theory Tech.*, vol. 37, pp. 953–961, June 1989.
[10] M. S. Viola, "A new electric field integral equation for heterogeneous dielectric bodies of revolution," *IEEE Trans. Microwave Theory Tech.*, vol. 43, pp. 230–232, Jan. 1995.
[11] D. H. Schaubert, D. R. Wilton, and A. W. Glisson, "A tetrahedral modeling method for electromagnetic scattering by arbitrarily shaped inhomogeneous dielectric bodies," *IEEE Trans. Antennas Propagat.*, vol. AP-32, pp. 77–85, Jan. 1984.
[12] A. W. Glisson and D. R. Wilton, "Simple and efficient numerical methods for problems of electromagnetic radiation and scattering from surfaces," *IEEE Trans. Antennas Propagat.*, vol. AP-28, pp. 593–603, Sept. 1980.
[13] A. K. Abdelmageed and K. A. Michalski, "Analysis of EM scattering by conducting bodies of revolution in layered media using the discrete complex image method," in *Proc. IEEE AP-S Int. Symp. Dig.*, vol. 1, 1995, pp. 402–405.

Andrzej A. Kucharski was born in Wroclaw, Poland, in 1964. He received the M.Sc. and Ph.D. degrees from the Wroclaw University of Technology Wroclaw, Poland, in 1988 and 1994, respectively.

Since 1993, he has been with the Radio Department, Institute of Telecommunications and Acoustics, Wroclaw University of Technology, where he is currently an Assistant Professor. During 1993 and 1994, he spent three months at the European Telecommunications Standards Institute, where he served as an expert in the field of satellite telecommunications. His research interests are primarily in computational electromagnetics, antennas and propagation, and electromagnetic compatibility.